

# Novel Spectral/Spatial Encoder Block for Incoherent Optical Multiple Access CDMA Networks

Mohamed RAHMANI<sup>1</sup>, Ghoutia Naima SABRI<sup>2</sup>, Abdelhamid CHERIFI<sup>3</sup>

<sup>1</sup>The Information and Telecommunications Processing Laboratory (LTIT), Electrical Engineering Department, Faculty of Technology, TAHRI Mohamed University of Bechar, Bechar, Algeria

<sup>2</sup>The Information and Telecommunications Processing Laboratory (LTIT), Department of Material Sciences, Faculty of Exact Sciences, TAHRI Mohamed University of Bechar, Bechar, Algeria

<sup>3</sup>Technology of Communication Laboratory (LTC), University of Tahar Moulay, Saida, Algeria

E-mail: rahmani.mohamed@univ-bechar.dz

**Abstract** - The major challenges of optical code division multiple access (OCDMA) systems are to increase transmission capacity while primarily reducing phase-induced intensity noise (PIIN). In this study, a novel two-dimensional spectral/spatial Shift Zero Cross-Correlation (2D-SHIFTZCC) code has been proposed for non-coherent spectral amplitude coding (SAC) systems. The code is designed in order to overcome the restraints of one-dimensional codes such as system complexity, and multiple access interferences (MAI), as well as enhance system capacity and accommodate a high data rate. For high cardinality, the numerical calculation shows that the proposed code (2D-SHIFTZCC) outperforms existent two-dimensional code families such as Perfect Difference (2D-PD), Diluted Perfect Difference (2D-DPD), Dynamic Cyclic Shift (2D-DCS), and Multi-Diagonal (2D-MD) codes regarding bit error rate (BER), and signal to noise ratio (SNR) when the number of available users, data rate, and transmitted power are considered.

**Keywords** – OCDMA , PIIN , SHIFTZCC , SAC.

## I. INTRODUCTION

Due to low attenuation, large bandwidth, and high data rate when employing light waves as a transmission tool between transmitter and receiver, optical networks can be created for long-distance transmission and display good transparency in communication protocols [1],[2].

This boosts the network's flexibility and functionality, and it fulfills the future requirements of optical networks, whether wired or wireless [3],[4]. Most networks are currently based on various multiple access techniques that allow multiple users to exchange data in the same channel simultaneously, such as time (TDMA: Time-Division Multiple Access), frequency (FDMA: Frequency Division Multiple Access), wavelength (WDMA: Wavelength Division Multiple Access), and spread coding (CDMA: Code Division Multiple Access). These multiplexing approaches increase system

capacity and can be adopted in future optical network generations [5].

Optical Code Division Multiple Access (OCDMA) is a popular optical communications approach that uses a spread spectrum of bit sequences as an encoding technique [2]. Additionally, the OCDMA network enables numerous users to transfer their resources to multiple optical receivers concurrently, synchronously, and asynchronously in the same medium, where each user has a unique signature on the same frequency spectrum and at the same time [6]. Furthermore, this multiplexing technology is distinguished by its great resilience to localized disturbances, which enables a variety of benefits such as high data rate, high power spectral density (DSP), and high transmission security.

The optical source divides the OCDMA scheme into two categories: coherent and incoherent systems. Overall, incoherent optical

encoders employing unipolar bits ("1" and "0") allow the codes to be not precisely orthogonal, resulting in the emergence of multi-access interferences (MAI) that completely dominate the system. Coherent systems based on bipolar bits ("1" and "-1") establish codes with good orthogonality that totally wipes out the effects of multi-access interference (MAI) [6-8].

The fundamental issue of OCDMA multiplexing technology is high phase-induced intensity noise (PIIN), which is generated by multi-user chip interference, resulting in multi-user interference (MUI), which primarily leads to system performance damage [8]. Since encoding and decoding are handled by simpler, cheaper, and less power-consuming components, Spectral Amplitude Coding (SAC) is a preferred approach mostly used in OCDMA networks. This makes the system flexible and efficient. Several codes have been developed to overcome PIIN noise and improve system performance, [9] developed one-dimensional multi-diagonal (1D-MD) code, in [10] one-dimensional dynamic cyclic shift (DCS) has been suggested, in [11] one-dimensional diagonal eigenvalue unit (1D-DEU) has been constructed, in [12] a new one-dimensional zero cross-correlation code (1D-NZCC) has been designed ...etc. However, due to the lengthier code size, which increases exponentially with the number of users, all of these codes limit cardinality and raise the complexity of detection at the receiver.

The frequency-spreading length is restricted to the optical pulse width and the delay precision of fiber-optic delay lines is preconditioned by the users' data rates since the cardinality of one-dimensional codes is proportional to the code length, i.e., the frequency-spreading length. Therefore, As a result, the cardinality (number of users) of one-dimensional unipolar codes that can be implemented is relatively small based on current state-of-the-art, and thus unipolar codes with higher cardinalities and better performances are required, so that OCDMA networks can support more simultaneous users. A significant amount of research work has identified the deployment of 2-D optical codes as one of the probable ways. The 2D optical codes do not

increase (reduce) code length while simultaneously increasing code size without decreasing performance. For example, multiple wavelengths or multiple optical fibers can be utilized as another encoding dimension to combine with the time dimension to form 2-D codes, such as 2-D wavelength-hopping/time-spreading codes (for short, wavelength-time codes), and 2-D wavelength-hopping/space-spreading codes.

Multiple two-dimensional procedures (spectral/spatial, spectral/time, spatial/time, etc.) have been explored for addressing the shortcomings of 1D codes involving code size and system ability. [13] suggested two-Dimension Perfect Difference code (2D-PD). In [14], a two-dimensional Hybrid Flexible Cross Correlation-Modified Double Weight (2D-FCC/MDW) is also proposed. Two-Dimensional Extended Enhanced Double Weight code (2D-EDW) has been proposed in [15]. In [16], two-Dimensional Dynamic Cyclic Shift is studied (2D-DCS). In [17], a two-dimensional Multi-Diagonal code (2D-MD) is developed. In [18], two-Dimensional Single Weight zero Cross Correlation (2D-SWZCC) is proposed to eliminate the PIIN effect. In [6] ,two-Dimensional Spectral/Spatial Code (2D-PTZCC) was proposed using the Pascal Triangle Rule for OCDMA System. In [5], Spectral / Spatial code (2D-HSSZCC) using Half-Matrix Technique is studied where the MAI effects are reduced thanks to the zero cross-correlation property. In [18], a novel 2D polarization-spatial encoding approach for the OCDMA system based on multi-core fiber (MCF) has been proposed. The system is developed to avoid the complexity of encoding and decoding methods, limit the nonlinearity effects by sharing the signal power between cores, and promote MCFs to enhance system security . In [19], a new algorithm to generate two-dimensional fixed right shifting (2D-FRS) code sequences is given. The proposed 2D-FRS algorithm is designed using 1D-FRS code with minimum cross-correlation (MCC). In [20], a new algorithm to generate two-dimensional (2D) encoding utilizing permutation vectors (PV) theory for

incoherent multiple access networks to suppress MAI and system complexity has been presented.

In this regard, the present investigation recommends a new two-dimensional Shift Zero Cross-Correlation (2D-SHIFTZCC) code characterized by good flexibility of code weight and the number of users, high management of adding/removing users, and simpler construction that renders the system simpler and consumes less power due to direct spectral detection at the receiver. Furthermore, the proposed code's performance is evaluated by comparing it to newly developed codes such as 2D-PD, 2D-DCS, 2D-DPD, and 2D-MD, where the proposed code reduces the complexity of the 2D system while achieving better performance in terms of available users, effective power, data rate, and spectral occupancy.

The rest of this work is organized as follows: the second section details the development of a new two-dimensional 2D-SHIFTZCC code, the third section provides a mathematical analysis in terms of SNR and BER expressions, and the fourth section presents and discusses the results obtained. Finally, in the fifth section, the conclusion relating to the effectiveness of the 2D-SHIFTZCC code is stated.

## II. CODE DESIGN

### A) One dimensional code

An optical code is typically denoted by  $(K, N, W, \lambda_a, \lambda_c)$  where  $K$  is the number of active users,  $N$  is the code length ( $N = K \times W$ ),  $W$  is the code weight,  $\lambda_a$  is autocorrelation, and  $\lambda_c$  is cross-correlation. The 1D-SHIFTZCC code was created in [21], and its construction is described in three stages:

#### Stage 1: Creating the merged matrix

We choose two matrices: one is an identity matrix ( $I_M$ ), and the other is a null matrix ( $N_M$ ) of the same dimension as the identity matrix. It should be noted that the number of matrices used and the dimension of the identity matrix are both equal to the weight value considered and the number of active users respectively. For example, when  $K = 3$  and  $W = 2$ , we obtain:

$$I_M = \begin{bmatrix} 1 & 0 & 0 \\ 0 & 1 & 0 \\ 0 & 0 & 1 \end{bmatrix} \text{ and } N_M = \begin{bmatrix} 0 & 0 & 0 \\ 0 & 0 & 0 \\ 0 & 0 & 0 \end{bmatrix} \quad (1)$$

As a consequence, the merged matrix ( $M_M$ ) is as follows:

$$M_M = \begin{bmatrix} 1 & 0 & 0 & 0 & 0 & 0 \\ 0 & 1 & 0 & 0 & 0 & 0 \\ 0 & 0 & 1 & 0 & 0 & 0 \end{bmatrix} \quad (2)$$

**Stage 2:** For each sequence, use the following technique to shift '1' to the right in the combined matrix:

$$S = W \times l - W - l + 1 \quad (3)$$

Where  $l$  is the corresponding line number,  $W$  is the weight of the code.

$$\begin{aligned} l_1 &= [1 \ 0 \ 0 \ 0 \ 0 \ 0] \\ \rightarrow l_1 &= [1 \ 0 \ 0 \ 0 \ 0 \ 0] \\ l_2 &= [0 \ 1 \ 0 \ 0 \ 0 \ 0] \\ \rightarrow l_2 &= [0 \ 0 \ 1 \ 0 \ 0 \ 0] \\ l_3 &= [0 \ 0 \ 1 \ 0 \ 0 \ 0] \\ \rightarrow l_3 &= [0 \ 0 \ 0 \ 0 \ 1 \ 0] \end{aligned}$$

#### Stage 3: Replacement

Replace the right zeros "W-1" with "1" to the right of each sequence's existing pulse. An example of 1D-SHIFTZCC code is given in Table 1 when  $K = 3$  and  $W = 2$ .

$$\begin{aligned} l_1 &= [1 \ 0 \ 0 \ 0 \ 0 \ 0] \\ \rightarrow l_1 &= [1 \ 1 \ 0 \ 0 \ 0 \ 0] \\ l_2 &= [0 \ 0 \ 1 \ 0 \ 0 \ 0] \\ \rightarrow l_2 &= [0 \ 0 \ 1 \ 1 \ 0 \ 0] \\ l_3 &= [0 \ 0 \ 0 \ 0 \ 1 \ 0] \\ \rightarrow l_3 &= [0 \ 0 \ 0 \ 0 \ 1 \ 1] \end{aligned}$$

TABLE 1. 1D-SHIFTZCC CODE

User	1D-SHIFTZCC code
$K_1$	1 1 0 0 0 0
$K_2$	0 0 1 1 0 0
$K_3$	0 0 0 0 1 1

### B) Two dimensional code

The 2D-SHIFTZCC code is derived from the 1D-SHIFTZCC code and can be built by combining two code sequences X, and Y, where X and Y represent spectral and spatial sequences, respectively. Let  $X_g$  represent  $[x_0, x_1, \dots, x_{l_1-1}]$  and  $Y_h$  represent  $[y_0, y_1, \dots, y_{l_2-1}]$  be two 1D-SHIFTZCC sequences.  $P_1$  and  $P_2$  are their code weights.  $l_1 = P_1 \times C_1$  is the spectral length, and  $l_2 = P_2 \times C_2$  is the spatial length, where  $C_1$  and  $C_2$  are the X and Y cardinalities.

The construction of 2D-SHIFTZCC can be stated as follows [3,4]:

$$A_{g,h} = Y_h^T X_g \quad (4)$$

Furthermore, in order to eliminate the influence of MAI in 2D-SHIFTZCC, we define four characteristic matrices  $A^{(d)}$ , where  $d \in (0,1,\dots,3)$  [6,22]:

$$\begin{cases} A^{(0)} = Y^T X \\ A^{(1)} = Y^T \bar{X} \\ A^{(2)} = \bar{Y}^T X \\ A^{(3)} = \bar{Y}^T \bar{X} \end{cases} \quad (5)$$

Table 2 displays the proposed code sequence designated by  $A_{g,h}$  in (4). Table III explains the new 2D-SHIFTZCC code's cross-correlation property, which is as follows:

$$R^{(d)}(g, h) = \sum_{i=0}^{l_1-1} \sum_{j=0}^{l_2-1} a_{i,j}^{(d)} a_{(i+g)(j+h)} = \begin{cases} P_1 P_2 & \text{when } g = 0 \cap h = 0 \\ 0 & \text{else} \end{cases} \quad (6)$$

TABLE 2. 2D-SHIFTZCC CODE FOR:  
( $P_1 = C_1 = P_2 = C_2 = 2$ )

	$X_0 =$ [1 1 0 0]	$X_1 =$ [0 0 1 1]
$Y_0^T =$ [1 1 0 0]	[1 1 0 0] [1 1 0 0] [0 0 0 0] [0 0 0 0]	[0 0 1 1] [0 0 1 1] [0 0 0 0] [0 0 0 0]

$Y_1^T =$ [0 0 1 1]	[0 0 0 0] [0 0 0 0] [1 1 0 0] [1 1 0 0]	[0 0 0 0] [0 0 0 0] [1 1 1 1] [1 1 1 1]
---------------------------------	--	--

TABLE 3. CROSS CORRELATION VALUE OF NEW 2D-SHIFTZCC CODE

	$R^{(0)}(g, h)$	$R^{(1)}(g, h)$	$R^{(2)}(g, h)$	$R^{(3)}(g, h)$
$g = 0 \cap h = 0$	$P_1 P_2$	0	0	0
$g = 0 \cap h \neq 0$	0	$P_1 P_2$	0	0
$g \neq 0 \cap h = 0$	0	0	$P_1 P_2$	0
$g \neq 0 \cap h \neq 0$	0	0	0	$P_1 P_2$

The developed 2D-SHIFTZCC code's cardinality and its length are represented as follows:

$$\begin{cases} C = C_1 \times C_2 \\ L = l_1 \times l_2 \end{cases} \quad (7)$$

### III. MATHEMATICAL ANALYSIS

Some hypotheses are presented in order to facilitate the analysis of the 2D-SHIFTZCC/OCDMA system: Firstly, the spectral spread of an unpolarized optical source is flat and broadband over the interval  $[v_0 - \Delta v/2, v_0 + \Delta v/2]$ , where  $v_0$  is the central frequency and  $\Delta v$  is the light source's bandwidth. Second, all of the data sent by each user to the receivers comes at the same time. Third and fourth, the power and spectrum width of each transmitter's spectral components are identical.

Overall, two main criteria are used to evaluate the performance of an optical system: bit error rate (BER), which is defined as the ratio of erroneous bits to transmitted bits, and signal-to-noise ratio (SNR), which is the ratio of received power to total noise power that affects the system. Furthermore, thanks to the zero cross-correlation (ZCC) feature of the 2D-SHIFTZCC code, user overlaps in the optical spectrum are completely ignored, removing the effect of multiple access interference (MAI). Thermal noise, shot noise, and phase-induced intensity noise (PIIN) are all discussed in this

context. As a result, the SNR and total variance noise from the photodetector are stated as follows [2, 4]:

$$SNR = \frac{I^2}{\langle i_{noise}^2 \rangle} \quad (8)$$

$$\langle i_{noise}^2 \rangle = \langle i_{Th}^2 \rangle + \langle i_{Sh}^2 \rangle + \langle i_{PIIN}^2 \rangle \quad (9)$$

Following the aforementioned hypotheses, the power spectral density (PSD) of the received signal is written as follows [17],[20]:

$$r(v) = \frac{P_{sr}}{P_2 \Delta v} \sum_{w=1}^C d(W) \sum_{i=0}^{l_1-1} \sum_{j=0}^{l_2-1} a_{i,j}^{(0)} a_{i,j}(w) \Pi(v, i) \quad (10)$$

$P_{sr}$ ,  $\Delta v$ , and  $\Pi(v, i)$  are the effective received power, optical bandwidth, and the  $i^{th}$  spectral element of the broadband source (BBS) respectively. Where  $\Pi(v, i)$  is defined as [3]:

$$\Pi(v, i) = \left\{ u \left[ v - v_0 - \frac{\Delta v}{2M} (-2l_1 + 2i) \right] - u \left[ v - v_0 - \frac{\Delta v}{2l_1} (-Ml_1 + 2i + 2) \right] \right\} = u \left[ \frac{\Delta v}{l_1} \right] \quad (11)$$

$u[v]$  is a unit step function defined as:

$$u(v) = \begin{cases} 1 & \text{when } v \in [0, +\infty[ \\ 0 & \text{when } v \in [-\infty, 0] \end{cases} \quad (12)$$

The photocurrent delivered by the photodiode (PD) at the receiver level can be expressed as:

$$I = \int_0^{+\infty} r(v) dv = \int_0^{+\infty} \frac{\mathcal{R} P_{sr}}{P_2 \Delta v} \sum_{w=1}^C d(W) \sum_{i=0}^{l_1-1} \sum_{j=0}^{l_2-1} a_{i,j}^{(0)} a_{i,j}(w) \Pi(v, i) \quad (13)$$

$$I = \int_0^{+\infty} r(v) dv = \frac{\mathcal{R} P_{sr}}{P_2 \Delta v} \int_0^{+\infty} (1 + 0) \times (P_1 P_2) \times \frac{\Delta v}{l_1} = \frac{\mathcal{R} P_{sr} P_1}{l_1} \quad (14)$$

$\mathcal{R}$  is the photodiode responsivity given as  $\mathcal{R} = \eta e / h \nu_0$ , where  $\eta$  is the quantum efficiency of the photodiode,  $h$  is Plank's constant and  $e$  is the electron charge.

The phase-induced intensity noise variance (PIIN) is calculated as follows [3]:

$$I_{PIIN}^2 = B_r I^2 \tau_C \quad (15)$$

Where  $B_r$  is electrical bandwidth,  $\tau_C$  is the light coherence time which is given as follows [3]:

$$\tau_C = \frac{\int_0^{+\infty} r^2(v) dv}{\left[ \int_0^{+\infty} r(v) dv \right]^2} \quad (16)$$

$$\begin{aligned} I_{PIIN}^2 &= B_r \mathcal{R}^2 \int_0^{+\infty} r^2(v) dv \\ &= B_r \mathcal{R}^2 \int_0^{+\infty} \left[ \frac{P_{sr}}{P_2 \Delta v} \sum_{w=1}^C d(W) \sum_{i=0}^{l_1-1} \sum_{j=0}^{l_2-1} a_{i,j}^{(0)} a_{i,j}(w) \right]^2 \Pi(v, i) \\ &= \frac{B_r \mathcal{R}^2 P_{sr}^2 \Delta v}{P_2^2 \Delta v^2 l_1} [(1 + 0) \times (P_1 P_2)]^2 \end{aligned}$$

Hence

$$I_{PIIN}^2 = \frac{B_r \mathcal{R}^2 P_{sr}^2 P_1^2}{\Delta v l_1} \quad (17)$$

Furthermore, thermal noise and shot noise are denoted as [7]:

$$I_{th}^2 = \frac{4K_b T_n B_r}{R_L} \quad (18)$$

$$I_{sh}^2 = 2e B_r I = 2e B_r \frac{\mathcal{R} P_{sr} P_1}{l_1} \quad (19)$$

Where  $I$ ,  $K_b$ ,  $T_n$ , and  $R_L$  are the average photocurrent, Boltzmann's constant, absolute temperature, and load resistor respectively.

Finally, the total noise is derived by substituting (17), (18), and (19) into (9) as:

$$\langle i_{noise}^2 \rangle = \frac{4K_b T_n B_r}{R_L} + 2e B_r \frac{\mathcal{R} P_{sr} P_1}{l_1} + \frac{B_r \mathcal{R}^2 P_{sr}^2 P_1^2}{\Delta v l_1} \quad (20)$$

Since the transmission of bits "1" and "0" is equally probable, the total noise becomes:

$$\langle i_{noise}^2 \rangle = \frac{4K_b T_n B_r}{R_L} + e B_r \frac{\mathcal{R} P_{sr} P_1}{l_1} + \frac{B_r \mathcal{R}^2 P_{sr}^2 P_1^2}{2 \Delta v l_1} \quad (21)$$

The expression of SNR is stated as follows based on the conclusions of (14) and (21).

$$SNR = \frac{I^2}{\langle i_{noise}^2 \rangle} = \frac{\left( \frac{\mathcal{R} P_{sr} P_1}{l_1} \right)^2}{\frac{4K_b T_n B_r}{R_L} + e B_r \frac{\mathcal{R} P_{sr} P_1}{l_1} + \frac{B_r \mathcal{R}^2 P_{sr}^2 P_1^2}{2 \Delta v l_1}} \quad (22)$$

As a result, the BER is determined from the SNR using Gaussian approximation and can be mentioned as [3,4]:

$$BER = \frac{1}{2} \operatorname{erfc} \sqrt{SNR/8} \quad (23)$$

#### IV. RESULTS AND DISCUSSION

The performance of the 2D-SHIFTZCC code is numerically examined in this part by comparing it to the two-dimensional codes PD, DPD, DCS, and MD given in [8,14,17,23],

where all codes have the same length. Table IV also illustrates the parameters adopted in the computational calculation. The performance of our suggested code is mainly assessed using two parameters, BER and SNR, in terms of the number of active users  $K$  and data rate  $R_b$ . Thermal noise, shot noise, and PIIN noise are also considered during the numerical calculation.

TABLE 4. ADOPTED PARAMETERS FOR NUMERICAL CALCULATION

Parameters	Value
Photo detector responsivity ( $\mathcal{R}$ )	0.65
Data rate ( $R_b$ )	1Gbps
Electric bandwidth ( $B_r$ )	$0.5 \times R_b$ GHz
Receiver Load resistor ( $R_l$ )	1030 $\Omega$
Spectral width of light ( $\Delta\nu$ )	3.75 THz
Effective source power ( $P_{sr}$ )	-10 dBm
Receiver noise Temperature ( $T_n$ )	300 K
Electron charge ( $e$ )	$1.6 \times 10^{-19}$ C
Boltzman's constant ( $K_b$ )	$1.38 \times 10^{-23}$ J/K

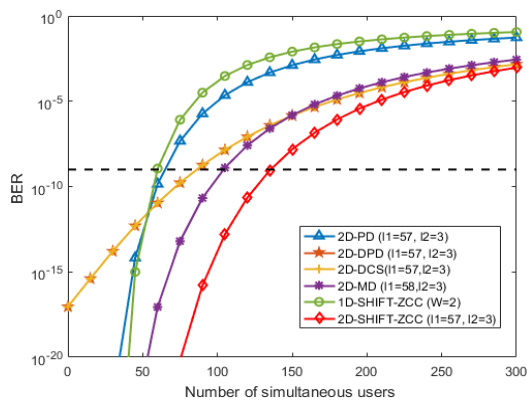


Fig. 1. BER regarding the concurrent subscribers.

Fig.1 plots the BER vs the number of active users when the effective source power and data rate are -10 dBm and 1 Gb/s, respectively, and the length of all codes is assumed to be the same. The 2D-SHIFTZCC code may reach 141 simultaneous users at a normalized  $BER = 10^{-9}$ , whereas the 1D-SHIFTZCC, 2D-PD, both 2D-DCS, 2D-DPD, and 2D-MD codes can reach 60, 66, 83, and 101, respectively. Consequently, the cardinality boosts 2.35 times when compared to 1D-SHIFTZCC, 2.13 times, 1.69 times, and 1.39 times when compared to 2D-PD, both 2D-DCS, 2D-DPD, and 2D-MD codes, respectively.

Consequently, the zero cross-correlation characteristic of the SHIFTZCC code explains this superiority, which restricts multiple access interference (MAI) and makes the system more suited for a large number of users.

Fig. 2 depicts the SNR effectiveness vs the number of active users when the data throughput is 1 Gb/s and the  $P_{sr}$  is -10 dBm. It's obvious that the signal-to-noise ratio is inversely related to the number of concurrent users; as the number of users increases, the signal-to-noise ratio decreases. The SNR reach of the 2D-SHIFTZCC code is 261 for a similar number of users equivalent to 100 users. Furthermore, SNR for 1D-SHIFTZCC, 2D-PD, both 2D-DPD, 2D-DCS, and 2D-MD codes can reach 51, 75, 133, and 148, respectively. As a result, the huge difference in SNR is justified by our 2D-SHIFTZCC code's ZCC attribute and lower noise power at the receiver.

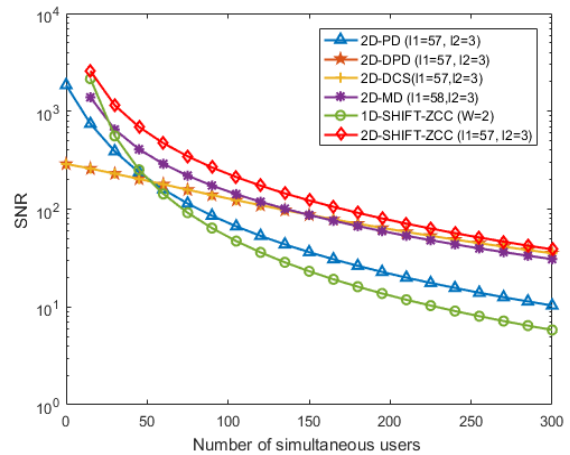


Fig. 2. SNR regarding cardinality.

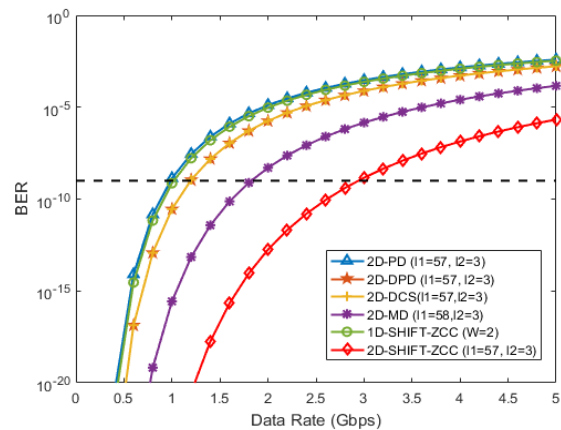
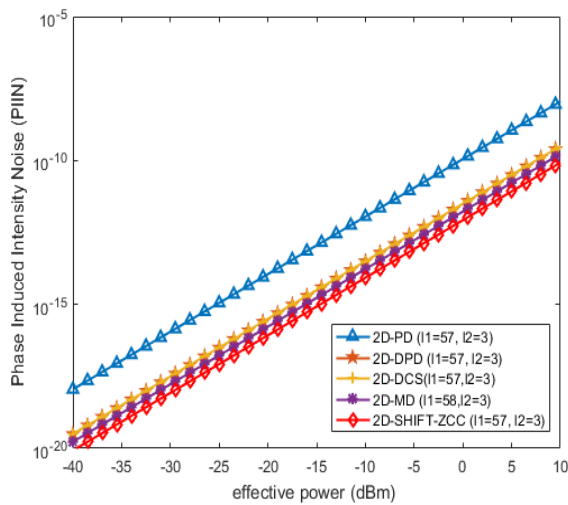


Fig. 3. BER versus data rate.

Fig. 3 depicts the BER curve versus data rate variation where the number of active users and effective source power are equal to 65 and -10 dBm, respectively, and all codes have the same length. Our 2D-SHIFTZCC code clearly accommodates a high data rate of 3.1 Gb/s, whereas the 1D-SHIFTZCC, 2D-PD, both 2D-DPD, 2D-DCS, and 2D-MD codes provide a data rate of 1.1, 1.02, 1.22, and 1.81 Gb/s at satisfactory  $BER = 10^{-9}$ . Thus, the proposed 2D-SHIFTZCC approach surpasses others and is compatible with systems capable of handling high data rates.



**Fig. 4.** PIIN noise regarding effective power.

Fig. 4 reveals the resulting PIIN noise curve as a function of transmitted power variation when the number of active users is set to 100 and all codes have the same spectral/spatial length. It is evident that the intensity of the noise PIIN increases according to the system's power. Furthermore, we note that our 2D-SHIFTZCC code has minimal PIIN noise after spectral detection at the photo-detector (PD) level, whereas the 2D-PD, 2D-DPD, 2D-DCS, and 2D-MD codes have an extremely high PIIN noise compared to the SHIFTZCC code. As a result of ZCC's ability to minimize PIIN noise, the suggested 2D-SHIFTZCC approach surpasses the others.

## V. CONCLUSION

A new two-dimensional spectral/spatial code family was established in this study. The 2D-SHIFTZCC code is modeled after a one-dimensional SHIFTZCC spread spectrum code in order to mitigate cross-correlation between any two separate users, diminish phase-induced intensity noise (PIIN), and disregard multiple access interferences (MAI). Each user is assigned a code word derived from a spectral code sequence and a spatial code sequence respectively. According to the numerical results, increasing the spatial code length improves system performance; additionally, the obtained results show that the 2D-SHIFTZCC performs better than the 2D-PD, 2D-DPD, 2D-DCS, and 2D-MD codes and increases system capacity by 2.35, 2.13, 1.69, and 1.39 times, respectively.

## VI. REFERENCES

- [1] M. Rahmani, A. Cherifi, G. N. Sabri, B. S. Bouazza, and A. Karar, "Contribution of OFDM modulation to improve the performance of non-coherent OCDMA system based on a new variable weight zero cross correlation code," *Opt Quant Electron*, vol. 54, no. 9, p. 576, Sep. 2022, doi: 10.1007/s11082-022-03949-5.
- [2] M. Rahmani, A. Cherifi, G. N. Sabri, M. I. Al-Rayif, I. Dayoub, and B. S. Bouazza, "A novel 260 Gb/s 2D-OCDMA-FSO multiplexing system's performance evaluation for upcoming generations of high-speed wireless optical networks," *Opt Quant Electron*, vol. 56, no. 3, p. 449, Mar. 2024, doi: 10.1007/s11082-023-05947-7.
- [3] M. Rahmani, A. Cherifi, A. S. Karar, G. Naima Sabri, and B. S. Bouazza, "Contribution of New Three-Dimensional Code Based on the VWZCC Code Extension in Eliminating Multiple Access Interference in Optical CDMA Networks," *Photonics*, vol. 9, no. 5, p. 310, May 2022, doi: 10.3390/photonics9050310.
- [4] M. Rahmani, A. Cherifi, G. Naima Sabri, M. I. Al-Rayif, I. Dayoub, and B. S. Bouazza, "Performance investigation of 1.5 Tb/s optical hybrid 2D-OCDMA/OFDM system using direct spectral detection based on successive weight encoding algorithm," *Optics & Laser Technology*, vol. 174, p. 110666, Jul. 2024, doi: 10.1016/j.optlastec.2024.110666.
- [5] M. Alayedi, A. Cherifi, A. F. Hamida, M. Rahmani, Y. Attalah, and B. S. Bouazza, "Design improvement to reduce noise effect in CDMA multiple access optical systems based on new (2-D) code using spectral/spatial half-matrix technique," *Journal of Optical Communications*, vol. 0, no. 0, p. 000010151520200069, Sep. 2020, doi: 10.1515/joc-2020-0069.

- [6] A. Cherifi, B. S. Bouazza, M. al-ayedi, S. A. Aljunid, and C. B. M. Rashidi, "Development and Performance Improvement of a New Two-Dimensional Spectral/Spatial Code Using the Pascal Triangle Rule for OCDMA System," *Journal of Optical Communications*, vol. 42, no. 1, pp. 149–158, Jan. 2021, doi: 10.1515/joc-2018-0052.
- [7] M. Alayedi, A. Cherifi, A. Ferhat Hamida, and H. Mrabet, "A fair comparison of SAC-OCDMA system configurations based on two dimensional cyclic shift code and spectral direct detection," *Telecommun Syst*, vol. 79, no. 2, pp. 193–212, Feb. 2022, doi: 10.1007/s11235-021-00840-8.
- [8] W. A. Intiaz, H. Y. Ahmed, M. Zeghid, and Y. Sharief, "An optimized architecture to reduce the impact of fiber strands in spectral/spatial optical code division multiple access passive optical networks (OCDMA-PON)," *Optical Fiber Technology*, vol. 54, p. 102072, Jan. 2020, doi: 10.1016/j.yofte.2019.102072.
- [9] T. H. Abd, S. A. Aljunid, H. A. Fadhil, R. A. Ahmad, and N. M. Saad, "Development of a new code family based on SAC-OCDMA system with large cardinality for OCDMA network," *Optical Fiber Technology*, vol. 17, no. 4, pp. 273–280, Jul. 2011, doi: 10.1016/j.yofte.2011.04.002.
- [10] T. Abd, S. Aljunid, H. Fadhil, R. Ahmad, and M. Junita, "Enhancement of performance of a hybrid SAC-OCDMA system using dynamic cyclic shift code," *Ukr. J. Phys. Opt.*, vol. 13, no. 1, p. 12, 2012, doi: 10.3116/16091833/13/1/12/2012.
- [11] H. Y. Ahmed and K. S. Nisar, "Diagonal Eigenvalue Unity (DEU) code for spectral amplitude coding-optical code division multiple access," *Optical Fiber Technology*, vol. 19, no. 4, pp. 335–347, Aug. 2013, doi: 10.1016/j.yofte.2013.04.001.
- [12] K. S. Nisar, H. Sarangal, and S. S. Thapar, "Performance evaluation of newly constructed NZCC for SAC-OCDMA using direct detection technique," *Photon Netw Commun*, vol. 37, no. 1, pp. 75–82, Feb. 2019, doi: 10.1007/s11107-018-0794-4.
- [13] Cheing-Hong Lin, Jingshown Wu, and Chun-Liang Yang, "Noncoherent spatial/spectral optical CDMA system with two-dimensional perfect difference codes," *J. Lightwave Technol.*, vol. 23, no. 12, pp. 3966–3980, Dec. 2005, doi: 10.1109/JLT.2005.859407.
- [14] N. D. Keraf, S. Aljunid, C. Rashidi, and P. Ehkan, "Performance of 2-D hybrid FCC-MDW code on OCDMA system with the presence of phase induced intensity noise," *ARNP J Eng Appl Sci*, vol. 11, no. 22, pp. 13203–8, 2016.
- [15] M. N. Nuroi, A. R. Arief, M. S. Anuar, S. A. Aljunid, N. Din Keraf, and S. Arif, "Performance analysis of 2-D Extended-EDW Code for optical CDMA system," in *2014 2nd International Conference on Electronic Design (ICED)*, Penang, Malaysia: IEEE, Aug. 2014, pp. 287–292. doi: 10.1109/ICED.2014.7015815.
- [16] N. Jellali, M. Najjar, M. Ferchichi, and H. Rezig, "Development of new two-dimensional spectral/spatial code based on dynamic cyclic shift code for OCDMA system," *Optical Fiber Technology*, vol. 36, pp. 26–32, Jul. 2017, doi: 10.1016/j.yofte.2017.02.002.
- [17] R. A. Kadhim, H. A. Fadhil, S. A. Aljunid, and M. S. Razalli, "A new two dimensional spectral/spatial multi-diagonal code for noncoherent optical code division multiple access (OCDMA) systems," *Optics Communications*, vol. 329, pp. 28–33, Oct. 2014, doi: 10.1016/j.optcom.2014.04.082.
- [18] A. Cherifi, N. Jellali, M. Najjar, S. A. Aljunid, and B. S. Bouazza, "Development of a novel two-dimensional-SWZCC – Code for spectral/spatial optical CDMA system," *Optics & Laser Technology*, vol. 109, pp. 233–240, Jan. 2019, doi: 10.1016/j.optlastec.2018.07.078.
- [19] S. Panda, "Effect of SHIFTZCC codes for optical CDMA system," *World scientific news*, vol. 2, no. 67, pp. 365–389, 2017.
- [20] M. Rahmani, G. N. Sabri, A. Cherifi, A. S. Karar, and H. Mrabet, "Massive capacity of novel three-dimensional OCDMA-FSO system for next generation of high-data wireless networks," *Trans Emerging Tel Tech*, vol. 35, no. 1, p. e4871, Jan. 2024, doi: 10.1002/ett.4871.